SEDIMENTOLOGY the journal of the International Association of Sedimentologists IAS

Sedimentology (2012) **59**, 1718–1734 doi: 10.1111/j.1365-3091.2012.01323.x

Magnetic mineral transport and sorting in the swash-zone: northern Lake Erie, Canada

ERIC GALLAWAY*, ALAN S. TRENHAILE*, MARIA T. CIOPPA* and ROBERT G. HATFIELD†

Department of Earth and Environmental Sciences, University of Windsor. Windsor, ON N9G 3P4, Canada (E-mail: tren@uwindsor.ca)

†College of Oceanic and Atmospheric Sciences, Oregon State University, Corvallis, OR 97331, USA

ABSTRACT

A combined field and laboratory study in northern Lake Erie has provided new insights into the origin and dynamics of heavy mineral placer deposits on beaches consisting primarily of non-magnetic sediment. Work was conducted on the cross-shore and longshore transport of heavy magnetic minerals using magnetic susceptibility and fluorescent paints to trace the movement, in the field, of samples of magnetic (magnetite) and non-magnetic (quartz and calcite) grains, respectively. Laboratory experiments examined how the burial of small, dense magnetic minerals is affected by the grain size of the non-magnetic host material, and how grain burial affects magnetic susceptibility measurements at the surface. The field experiments demonstrated that the magnetic mineral tracers were buried rapidly beneath coarser, non-magnetic grains under low to moderate wave conditions, and subsequently were unable to move in the longshore or cross-shore directions. The laboratory experiments showed that the magnetic susceptibility rapidly decreased with the rate and depth of burial of the magnetic minerals, and that magnetic grain burial was most effective beneath coarser rather than finer non-magnetic sand and, for the latter sediments, under less rather than more energetic conditions. The results imply that magnetic mineral concentrations develop in this area through magnetic grain burial under fairly mild conditions, and subsequent settling, exposure and concentration in the upper swash zone during more energetic periods, when the non-magnetic grains are eroded. It is probably during these erosional periods, when the magnetic minerals are exposed in fairly homogeneous deposits, that longshore and cross-shore transport takes place.

Keywords Beaches, magnetic minerals, magnetic susceptibility, placers, sorting, tracers.

INTRODUCTION

Beach sediment sorting is the result of a number of variables working together, or independently, to separate grains with different characteristics. These variables include the rate of sediment accumulation, nature of the sediment surface, mode of grain movement, flow depth, velocity and other characteristics, and the size, shape and density of the grains (Steidtmann, 1982). Sediment sorting is sensitive to variations in grain density, and particularly to the abundance and mineralogy of the heavy mineral component. Consequently, heavy minerals, which are often magnetic, are frequently concentrated in beach placers, sand dunes and beach ridges (Komar & Wang, 1984; Peterson *et al.*, 1986; Li & Komar, 1992a,b; Frihy *et al.*, 1995; Hughes *et al.*, 2000; McCubbin *et al.*, 2000; Hou *et al.*, 2003; Bryan *et al.*, 2007). Heavy minerals accumulate on beaches in bands or streaks near the high tidal level or in the upper swash zone, as well as in the troughs of ripples and where there are shells, coarse clasts or other flow obstructions (Li &

Komar, 1992a; Frihy *et al.*, 1995). Viewed in cross-section, the upper swash zone frequently consists of layers of fine, heavy minerals, grading upwards into layers of coarser sediment. These alternating layers are between *ca* 1 mm and 25 mm in thickness, and they typically extend along the beach for a few tens of metres (Clifton, 1969).

It has been assumed that because small, heavy mineral grains are shielded from the flow by larger quartz and other grains, they are less easily entrained and therefore are carried alongshore less rapidly than the larger, less dense grains, even when they have the same fall velocity (Slingerland, 1977; Trask & Hand, 1985). Heavy mineral concentrations in the cross-shore direction have been attributed to heavy minerals being carried onshore by higher current velocities, but not by the weaker offshore flows (wave current asymmetry), or to beach erosion and offshore transport of the lighter, more easily mobilized grains (Komar & Wang, 1984). In the swash zone, it has been proposed that shear sorting by swash and backwash causes the coarser, or lighter, grains to migrate upwards into the zone of lower shear, whereas the finer, or heavier, grains move downwards, into the zone of maximum shear at the bed. Alternately, smaller particles may tend to fall into the spaces between the larger grains, thereby displacing coarser grains towards the surface, a process that has been termed kinetic sieving (Clifton, 1969; Sallenger, 1979; Komar & Wang, 1984; Hughes *et al.*, 2000; Tomkins *et al.*, 2010).

The analysis of heavy magnetic minerals has been used in coastal environments to determine the chronology of pollution and deposition in estuaries, salt marshes and tidal flats, and to investigate sediment provenance, transport paths and depositional processes (Foster *et al.*, 1991; Razjigaeva & Naumova, 1992; Oldfield & Yu, 1994; Lees & Pethick, 1995; Wheeler *et al.*, 1999; Lario *et al.*, 2001; Kean, 2004; Plater & Appleby, 2004; Booth *et al.*, 2005; Zhang *et al.*, 2007; Maher *et al.*, 2008; Rotman *et al.*, 2008; Cioppa *et al.*, 2010). Along the Nile Delta, Frihy *et al.* (1995) and Frihy & Dewidar (2003) distinguished areas of erosion with a concentration of heavier and denser minerals and areas of deposition with a higher proportion of lighter minerals. More recently, Hatfield *et al.* (2010) conducted a similar study based on the distribution of heavy magnetic minerals along the beaches of eastern Point Pelee, in north-western Lake Erie, Canada.

Heavy mineral deposits often contain significant concentrations of magnetite and other ferromagnetic oxides (Hatfield *et al.*, 2010). Magnetic techniques are potentially useful tools for coastal investigations; however, sufficient understanding of the mechanisms responsible for magnetic mineral sorting, concentration and transportation on the foreshore is presently lacking. To further understanding of the behaviour of magnetic material on beaches dominated by non-magnetic grains, a study was conducted to examine the movement of magnetic sediment in the swash zone along the north-western coast of Lake Erie. This study built on previous work in this area that used magnetic properties to trace sand sources and transport paths and to identify areas of accelerated beach erosion (Cioppa *et al.*, 2010; Hatfield *et al.*, 2010). Those investigations raised questions regarding modes and rates of magnetic mineral transport in this area. The present study was designed to:

1 Investigate spatial and temporal variations, and the processes responsible for them, in the cross-shore and longshore transport of heavy magnetic grains.

2 Determine whether there is a relationship between the transport of magnetic and non-magnetic grains and whether, if there is a relationship, magnetic susceptibility measurements can be used to estimate rates of longshore transport of dominantly, non-magnetic minerals.

3 Study the origin of heavy mineral placer deposits.

THE STUDY AREA

The study was conducted on the eastern side of Point Pelee, a large cuspate foreland on the north-eastern shore of Lake Erie in southern Canada. Point Pelee extends *ca* 15 km into Lake Erie, with the southern 9 km forming Point Pelee National Park (PPNP; Fig. 1). The eastern coast consists of a thin barrier beach, consisting of fine-grained to coarse-grained sand, which protects fragile marshy ecosystems from wave attack. It has been estimated that annual erosion rates were between 0·4 m and 2·8 m along the eastern barrier beach between 1918 and 1973 (Coakley, 1980) and that southerly, alongshore transport rates were between 6000 m^3 $year^{-1}$ and 19 000 m^3 $year^{-1}$ (Kamphuis, 1972; Skafel *et al.*, 1985; Trenhaile *et al.*, 2000); transport rates have probably declined in recent years owing to the construction of permanent structures along the north-eastern

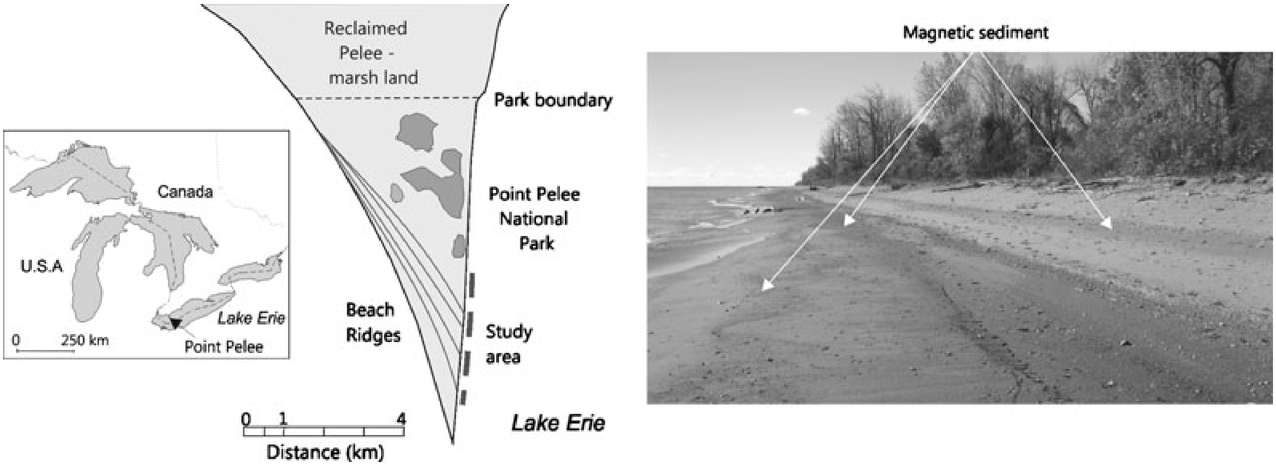

Fig. 1. The study area along the south-eastern coast of Point Pelee, north-western Lake Erie. The photograph shows a primarily sandy foreshore with bands or streaks of dark, magnetic sediment. The beach is *ca* 30 m wide in this area.

flanks of PPNP (Trenhaile *et al.*, 2000). The width of the beach ranges from 3 m to more than 40 m along eastern Point Pelee. The beach is narrower and more variable in the north, where it runs along the edge of the marsh, than in the south where it fronts ridge and swale complexes and Carolinian forest. Work was conducted along this southern sector, on a fairly secluded section of the beach extending *ca* 1 to 5 km from the tip.

Waves are most frequently generated from the south-west and north-west and are refracted into the study area around the tip of the Point. The longest fetches off Point Pelee are to the east and north-east, from which storms generate large destructive waves, especially during spring and autumn. Lake ice generally protects the shore in winter. Long-term coastal recession on the western side and recession on the eastern side are causing the Point to gradually pivot westwards, producing a gentle submarine slope with a series of submarine bars off the eastern shore.

Although microscopy and X-ray diffraction analysis showed that the beach is dominated by grains of quartz and calcite, there are thick and extensive heavy mineral deposits in places that exhibit strong evidence of erosion, in the field and in the historical record (Cioppa *et al.*, 2010; Hatfield *et al.*, 2010; Fig. 1). Magnetic remanence measurements demonstrated that the magnetic properties are dominated by multi-domain ferromagnetic grains, probably magnetite and/or maghemite. Particle size-specific measurements also showed that the <250 μm fraction of the beach sands was responsible for the majority of the bulk magnetic signal (Hatfield *et al.*, 2010).

METHODS

Field experiments

Although this study was concerned with the transport of magnetic minerals in the swash zone, some experiments were also run, for comparative purposes, to investigate the movement of non-magnetic minerals. Movement of the magnetic minerals was tracked by recording changes in magnetic susceptibility, whereas fluorescent tracers and sediment coring were used to track the non-magnetic grains. Nineteen magnetic and two concurrent non-magnetic tracing experiments were conducted between July and November 2010. Another six non-magnetic tracing experiments, run without concomitant magnetic tracing, provided additional information on the movement of non-magnetic grains under similar conditions to those in the runs with magnetic tracing. Accompanying laboratory measurements were also undertaken to investigate grain sorting and magnetic mineral burial under controlled conditions.

Sand was removed from the beaches in the study area and air-dried. A rare-earth magnet was used to separate the magnetic and non-magnetic grains. The term 'non-magnetic' is used in this study to refer to the residual sand that had a weak magnetic moment and could not be extracted with the rare-earth magnet; and 'magnetic' is used for sand with a strong positive susceptibility that was extracted by the magnet. Two fluorescent paints were considered for the non-magnetic grains, an acrylic 'screen printing ink' manufactured by Speedball Art Products (Statesville, North Carolina, USA), and an alkyd enamel (oil paint) manufactured by Macdonald & White Varnish and Paint Company (Windsor, Ontario, Canada). Before any paint was applied, the non-magnetic sand was sieved to determine the grain-size distribution. The paints were thinned, using water for the acrylic paint and mineral spirits for the enamel paint, and then hand mixed with the sand. An equal volume of water and paint produced a solution with a consistency a little thicker than water, and a ratio of 200 ml of thinned paint to 900 g of sand produced just enough thinned paint to coat all the grains without leaving any excess within the mixture.

Tests were conducted to determine whether the paint applications satisfied the fluorescent tracer criteria of Yasso (1966); these include requirements that the coat of paint on the sand grains should be thin, so that it does not markedly alter the hydrodynamic behaviour of the grains, and resistant to abrasion and dissolution in water. The painted sand was air-dried for 16 h and then oven-dried for 2 h at 70°C. After drying, the sand was placed in a sieve-shaker for 1 h to determine the modified grain-size distribution and to break up any clumps that may have developed. The mean (all the means given in this study are arithmetic rather than geometric) and median grain size, skewness and kurtosis were then compared with the same parameters for the original, pre-painted grain-size distribution (Fig. 2). Although the application of the acrylic paint did increase the non-magnetic grain size, the effect was much lower than for the enamel paint; the testing procedure was repeated three times to ensure that the results were consistent. To ensure that the acrylic coat was also resistant to abrasion and dissolution, the sand was placed in a pan with water and shaken for 1 h. After drying, the sand was placed under ultraviolet light to confirm that the grains were still fluorescent and could be distinguished from unpainted grains. Different acrylic colours were used for the non-magnetic material, according to the grain size – green for grains <250 μm (mean 209 μm) and pink for grains >250 μm (mean 483 μm); the former tracers are subsequently referred to in this study are referred to as the finer non-magnetic tracers and the latter as the coarser non-magnetic tracers. This distinction between the two non-magnetic tracers allowed a direct comparison to be made between magnetic and finer non-magnetic grains of roughly the same size, based on the observation that heavy magnetic grains in

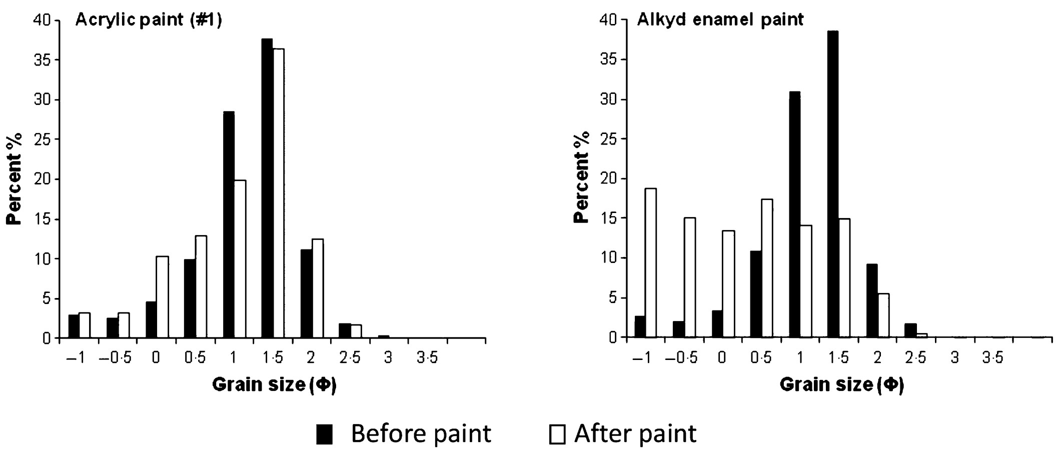

	Acrylic (1)		Acrylic (2)		Acrylic (3)		Enamel	
	Before	After	Before	After	Before	After	Before	After
Mean	0·90	0·77	1·02	0·90	1·01	0·95	0·92	0·04
Median	1·00	1·00	1·15	1·00	1·10	1·07	1·00	0·01
Skewness	–0·16	–0·31	–0·18	–0·13	–0·14	–0·16	–0·12	0·02
Kurtosis	1·45	1·05	1·14	1·00	1·31	1·12	1·42	1·17
Sorting	0·64	0·75	0·69	0·76	0·66	0·71	0·62	1·10

Fig. 2. Pre-painted and post-painted grain-size distributions and statistical summary data for three acrylic-paint tests and one enamel-paint test.

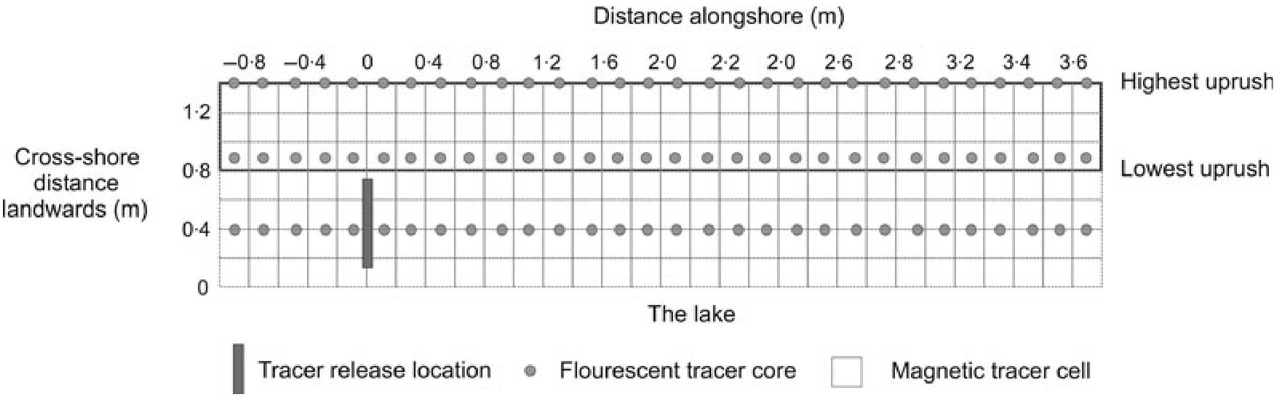

Fig. 3. The sampling grid showing the cells used to measure magnetic susceptibility and to take core samples for the fluorescent tracers. The grid extended 7 m downdrift and 2 m updrift but is shown in a truncated form here.

the study area are primarily <250 µm in size (Hatfield *et al.*, 2010) (the mean grain size of the magnetic tracers was 178 µm).

Tracer movement in the swash zone was measured using markers placed at 0·2 m intervals along the beach, landwards of the maximum swash uprush, for 7 m in the downdrift direction and 2 m in the updrift direction (Fig. 3). The length of this experimental track was based on preliminary experiments which showed that there was little movement of the tracers beyond these boundaries during the several hours of each experiment. The magnetic and non-magnetic tracers were saturated with water in a bag before being released into the swash zone. The width of the surf zone determined the amount of magnetic tracer that was used: 750 g when <3 m; 1500 g when 3 to 5 m; and 3000 g when >5 m. For the non-magnetic tracer experiments, 750 g of the green and 750 g of the pink tracer were used when the width of the swash zone was <3 m and 1500 g of each was used when the swash zone was >3 m.

Longshore and cross-shore magnetic susceptibility measurements were made in the field with a Bartington MS2 susceptibility meter (Bartington Instruments Ltd, Witney, UK) with a 0·2 m diameter D probe. Consequently, all measurements were made within 0·2 m square cells (Fig. 3), the cross-shore measurements being taken by carefully reaching over the swash zone to avoid trampling on it and disturbing the grain distributions. The one exception to this procedure was in magnetic tracer Run 18, which had a 6 m wide swash zone. Because the researcher would have had to enter, and therefore disturb, this wide swash zone during the experiment to take sample readings, the distribution of the tracers was recorded only at the end of this experiment.

The background magnetic susceptibility was recorded in each of the cells immediately preceding each magnetic tracing experiment. The magnetic tracers were then distributed evenly along the 0 m marker, extending from the minimum extent of the uprush to *ca* 0·4 to 1 m lakewards, depending on the breaker height and swash zone width. Magnetic susceptibility measurements were then made in each cell at intervals ranging from 15 to 30 min, for up to 3·5 h, depending on rates of movement and grain burial.

The non-magnetic tracers were released into the swash zone in the same way as for the magnetic tracers. The movement of these grains was recorded by extracting sediment cores in glass containers, 15 mm in diameter and 50 mm deep, at 0·2 m intervals alongshore and at 500 mm intervals cross-shore. Core collection was made only at the end of each experiment because of its invasive nature and inevitable disturbance of the sand. The cores were examined under an ultraviolet light in the laboratory to determine the number and depth of the fluorescent grains in each core. To minimize disturbance, including changes in tracer depth that might have arisen from drying, the number of fluorescent grains of each colour was counted only from the outer perimeter of the cores (although not from the top or bottom surfaces), through the glass container. The number of tracer grains in each core, of each of the two size categories, was represented as a percentage of the total number of the same tracers identified in all the cores.

Breaker height and period and swash direction and uprush velocity were recorded during the experiments, as well as the gradient, width and grain size of the swash zone (Table 1). Breaker height and swash zone width were measured

Table 1. Summary of the run conditions and tracer movement.

Run	Mean grain size (mm)	Swash angle (°)	Swash width (m)	Swash zone gradient (°)	Breaker height (m)	Breaker period (s)	Swash velocity (m s^{-1})	Breaker type	Tracer alongshore velocity (m h^{-1})	Tracer cross-shore (%)
1	1·25	0·0	1·6 to 1·2	9·1	0·23 to 0·17	1·8	0·5	Plunging	0·01	76·1
2	0·66	2·0 to −0·7	2·0 to 1·3	7·8	0·37 to 0·23	3·7	0·6	Plunging	0·17	72·8
3	2·80	8·0 to 6·0	1·8 to 1·3	4·7	0·20 to 0·13	4·5	0·6	Plunging	0·09	63·6
4	0·54	4·0 to 0·7	1·5 to 0·9	6·4	0·11 to 0·08	2·4	0·5	Plunging	0·11	85·8
5	1·08	2·0 to −0·7	1·8 to 0·9	6·4	0·22 to 0·15	2·3	0·7	Plunging	0·12	70·7
6	2·07	0·0	1·8 to 1·2	9·4	0·21 to 0·11	2·9	0·7	Surging	0·03	61·7
8	0·81	2·0 to 1·0	1·2 to 0·8	9·0	0·09 to 0·06	4·6	0·5	Surging	0·05	75·4
9	0·56	6·5 to 6·0	2·8 to 1·6	8·3	0·26 to 0·15	3·3	0·9	Surging	0·22	66·6
10	1·20	5·3 to 3·0	1·7 to 1·0	8·9	0·26 to 0·13	2·3	0·8	Plunging	0·16	53·5
11	0·99	4·0	2·1 to 1·2	6·4	0·20 to 0·13	3·0	0·6	Plunging	0·12	66·5
12	0·33	2·7 to 1·3	1·8 to 1·0	6·9	0·1	4·5	0·5	Surging	0·04	53·5
14	0·69	8·0 to 6·0	3·5 to 2·6	6·9	0·53 to 0·30	3·6	1·0	Plunging	0·11	67·1
15	0·75	8·0	3·6 to 2·8	8·5	0·80 to 0·30	3·3	1·1	Plunging	0·80	83·2
16	1·04	10·0 to 8·0	4·0 to 2·6	7·1	0·54 to 0·25	3·5	1·1	Plunging	0·72	74·4
17	0·47	2·7 to −0·7	2·7 to 1,6	8·6	0·32 to 0·21	2·2	1·1	Plunging	0·18	82·5
18	0·52	2·0 to −2·0	6·0 to 4·0	5·0	1·00 to 0·50	3·5	1·5	Spilling	1·25	77·8
19	0·49	3·3 to 1·3	3·5 to 2·0	7·3	0·49 to 0·25	2·7	1·2	Plunging	0·79	75·2
20	0·38	2·0 to 0	3·0 to 1·8	7·7	0·60 to 0·40	2·4	0·9	Plunging	0·31	60·7
21	0·38	6·0 to 4·0	2·0 to 1·4	6·9	0·32 to 0·20	3·5	0·7	Plunging	0·30	45·8
A	0·35	6·0 to 5·0	1·6 to 1·3	6·5	0·30 to 0·18	3·2	0·6	Plunging	1·61/2·33	58·3/52·8
B	0·76	10	2·5 to 1·5	6·1	0·43 to 0·20	3·1	0·7	Plunging	2·67/2·58	69·1/60·0
C	0·54	8·0 to 6·0	2·3 to 1·7	6·6	0·31 to 0·18	3·0	0·7	Plunging	1,73/2·17	62·3/74·4
D	0·54	9·0 to 8·0	1·6 to 1·5	7·3	0·24 to 0·13	2·8	0·8	Plunging	2·63/2·31	71·4/68·4
E	1·00	6·0 to 5·0	1·5 to 0·9	7·9	0·15 to 0·12	3·5	0·5	Surging	0·70/1·00	67·4/72·5
F	0·81	6·0 to 5·0	2·2 to 1·5	7·9	0·15 to 0·12	3·2	0·5	Surging	1·07/1·43	68·5/76·2
G	0·38	2·0 to 0	3·0 to 1·8	7·7	0·60 to 0·40	2·4	0·9	Plunging	2·12/2·33	61·1/56·9
H	0·38	6·0 to 4·0	2·0 to 1·4	6·9	0·32 to 0·20	3·5	0·7	Plunging	2·59/2·56	64·9/65·9

Run numbers and letters refer to magnetic and non-magnetic experiments, respectively. Swash angle refers to the direction of the swash north (positive) and south (negative) of a line perpendicular to the shore. Experiments 20 and G, and 21 and H were run simultaneously. Alongshore velocity, which has two values for the non-magnetic tracers (smaller grains first, larger grains second), refers to the velocity during the first hour of the magnetic tracer experiments, and over the entire experimental period for the non-magnetic tracers. The cross-shore percentage (%) refers to the position of the tracers (two values for the smaller and larger non-magnetic tracers) at the end of the experiments, expressed as a percentage of the swash width measured in a landward direction.

with a tape, swash angle with a compass and breaker period with a stopwatch. Swash uprush velocity was estimated by timing the movement of a surface float over a fixed distance; this procedure was repeated 10 times and the velocities were averaged. The beach gradient was determined from the length of the vertical rise over the corresponding horizontal length. All these measurements were repeated every hour during the experiments. The swash zone grain-size distribution was obtained by sieving 0·5 to 1 kg sand collected from the surface, either side of the gridded measurement area, immediately before and after the experiments. All correlations between tracer movement and breaker, swash, and beach conditions were tested for significance at the 95% confidence level.

A spatial integration method was applied to each of the longshore tracer distributions (Crickmore & Lean, 1962; Komar & Inman, 1970; White & Inman, 1989; Ciavola *et al.*, 1997; Nordstrom *et al.*, 2003; Tonk & Masselink, 2005). The longshore velocity of the tracers, which refers to the movement of the centroid of the tracer cloud, was determined using the expression:

$$v = \frac{\sum_{(x,y)}^{N} N(x, y, t')x/t}{\sum_{(x,y)}^{N} N(x, y)}$$

where v is the velocity, N is the tracer concentration, x is the longshore distance from the location of tracer injection, y is the distance up the swash zone and t is the elapsed time since the tracer sample was released. Magnetic tracer concentrations were represented by the magnetic susceptibility values, using only values that were greater than the pre-experimental background values in the swash zone. For the non-magnetic tracers, the concentrations were represented by the number of grains of each colour that were counted along the perimeter of each core.

Because the dispersion of the magnetic and non-magnetic tracers was determined in different ways, the relative rates of movement could be influenced, to some degree, by the methods that were used. Therefore, only broad comparisons were made between the rates and distances of tracer movement, which were corroborated by visual observation of the dispersion of the black and coloured tracers during the early part of the experiments, before they were too diffused. Additionally, relationships between tracer movement and beach and wave conditions were made for each type of tracer, rather than for the combined data.

Laboratory experiments

To investigate the effect of grain burial on magnetic susceptibility measurements, 300 g of magnetic tracer was distributed in a layer, *ca* 1 mm thick, on top of non-magnetic sand in a 400×500 mm plastic box. The magnetic susceptibility was measured at six points on the surface to determine the mean value. A fixed volume of non-magnetic sand, equivalent to a 2 mm layer, was then laid evenly on top of the magnetic grains and the magnetic susceptibility at the surface was recorded again at the same six locations. This procedure was repeated as additional 2 mm thick layers of non-magnetic sand were added to the container; the experiment concluded when the magnetic layer had been buried under 84 mm of non-magnetic sand.

A second experiment was conducted in the laboratory to investigate the effect of the grain size of the non-magnetic host on magnetic sand burial rates. Non-magnetic sand from Point Pelee was sieved and separated into 2·83 to 2·00 mm (−1·5 to −1 φ), 0·93 to 0·71 mm (0·1 to 0·5 φ), 0·71 to 0·50 mm (0·5 to 1 φ) and 0·50 to 0·35 mm (1 to 1·5 φ) grain sizes. Each size fraction was poured into a cylindrical plastic container (diameter 300 mm) to a depth of 100 mm. Water was then added to each container until it was 10 mm above the top of the sand, and 100 g of magnetic tracer was then spread out evenly over the non-magnetic surface. The magnetic susceptibility was measured on the surface of each container at three points around the perimeter and at one point in the centre. The containers were shaken at a speed of 50 rotations per minute using an electric agitator for 1 min, and the magnetic susceptibility was then recorded at the same points on the sand surface. This process was repeated for 22 min at 1 min intervals. The same experimental procedure was then used to repeat the experiments with greater agitation, at 70 rotations per minute.

RESULTS

Field results

Longshore rates of transport of the magnetic tracers decreased though time in almost all of the experiments. Rates of movement, which were commonly more than 1 m h^{-1} over the first 10 min of the experiments, were usually <0·1 m h^{-1} after 1 to 2 h. Tracer movement had stopped completely after a few hours in about half the runs, and by the next morning in most others (Fig. 4). Movement generally continued for longer in runs with higher breakers than in those with lower breakers. In the cross-shore direction, the magnetic tracers moved landwards during all the experiments, generally into the upper 60 to 80% of the surf zone (Table 1). The longshore velocity of the finer non-magnetic tracers was between 0·70 m h^{-1} and 2·67 m h^{-1}, and between 1·00 m h^{-1} and 2·58 m h^{-1} for the coarser non-magnetic tracers. In combined experiments Run 20 and Run G, which employed both magnetic and non-magnetic tracers, the magnetic tracers had a mean longshore velocity over the first hour of 0·31 m h^{-1}, compared with 2·12 m h^{-1} and 2·33 m h^{-1} for the finer and coarser non-magnetic tracers, respectively. The corresponding figures in concurrent Runs 21 and H, which also used magnetic and non-magnetic tracers, were 0·30 m h^{-1}, 2·59 m h^{-1} and 2·56 m h^{-1}, respectively (Table 1; Fig. 5).

There was one clear exception to the general decrease in alongshore velocity. In Run 3, once the longshore movement of the magnetic tracer centroid had fallen to *ca* 0·12 m h^{-1}, which occurred after *ca* 37 min, it continued to move alongshore at this velocity for the next 113 min (Fig. 4); it is not known whether the magnetic tracers continued to move alongshore after that time. The reason for protracted longshore transport in this run is unclear, particularly as its only distinguishing characteristics were the coarse surface sediment (2·80 mm), which should have

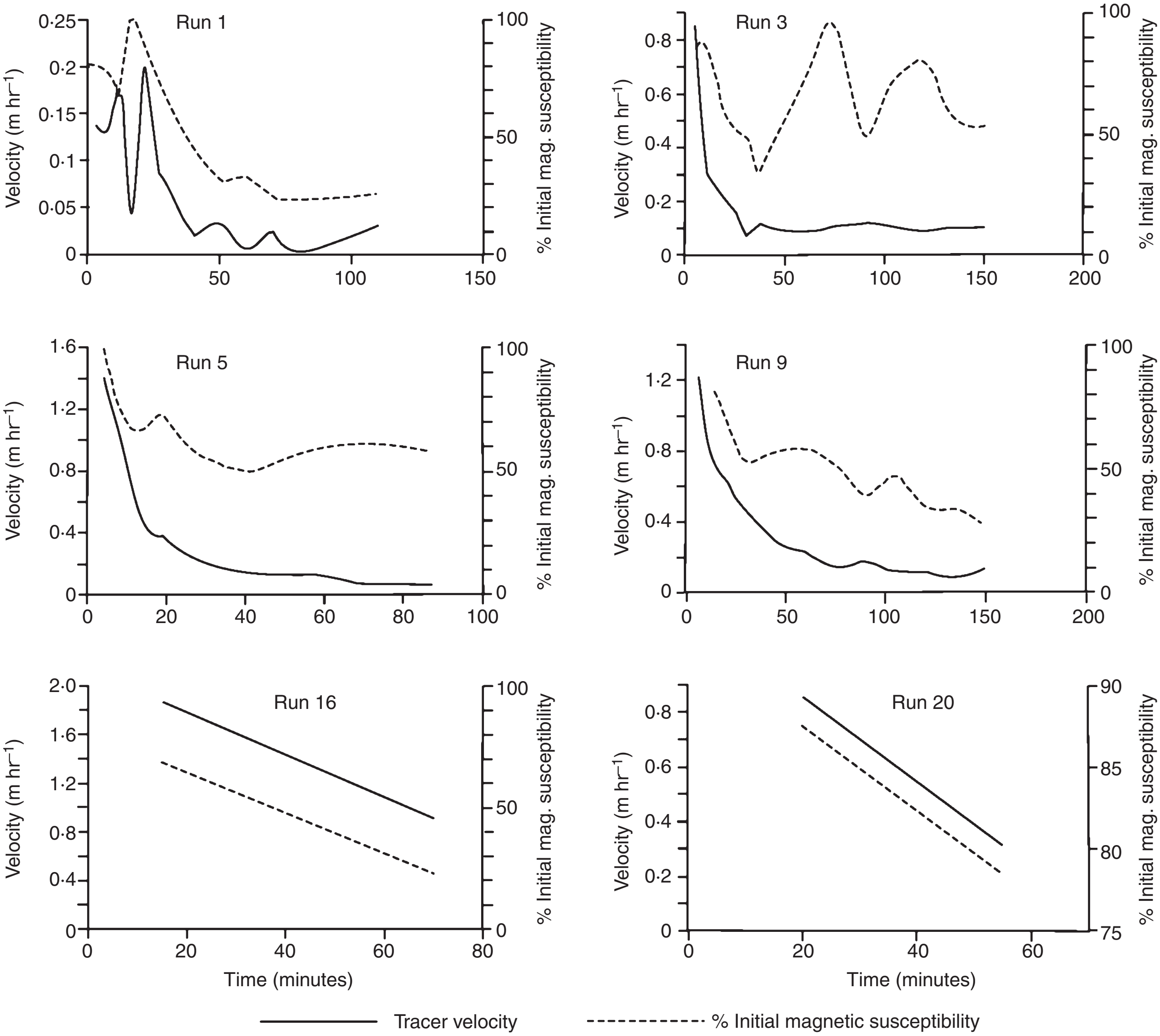

Fig. 4. Examples of experiments showing changes in the rate of longshore movement of the magnetic tracer centroid and in the total magnetic susceptibility.

promoted magnetic grain shielding and burial, and the low swash zone gradient (Table 1).

Because higher-energy conditions were less frequent than lower-energy conditions over the experimental period, the distributions of such variables as breaker height, swash velocity and rates of transport had a positive skew. Log-log and log-linear transformations were made to the data to produce more normal distributions for the correlation and regression analyses. Additionally, because rates of movement of the magnetic tracers decreased through time, only the movement over the first hour of the experiments was used to analyse relationships with various experimental conditions. As coring was only conducted at the end of the experiments, correlations were made between the movement of the non-magnetic tracers and prevailing conditions over the entire experimental periods.

There were significant, moderate to high correlations between the log of the longshore tracer velocity and the log of the breaker height for all three tracers, and between the log of the longshore tracer velocity and the swash (uprush) velocity for the magnetic and finer non-magnetic tracers (Fig. 6). None of the correlations between longshore velocity and breaker period and swash angle were significant. There was also a high, significant correlation between the cross-shore position (percentage distance of the centroid up

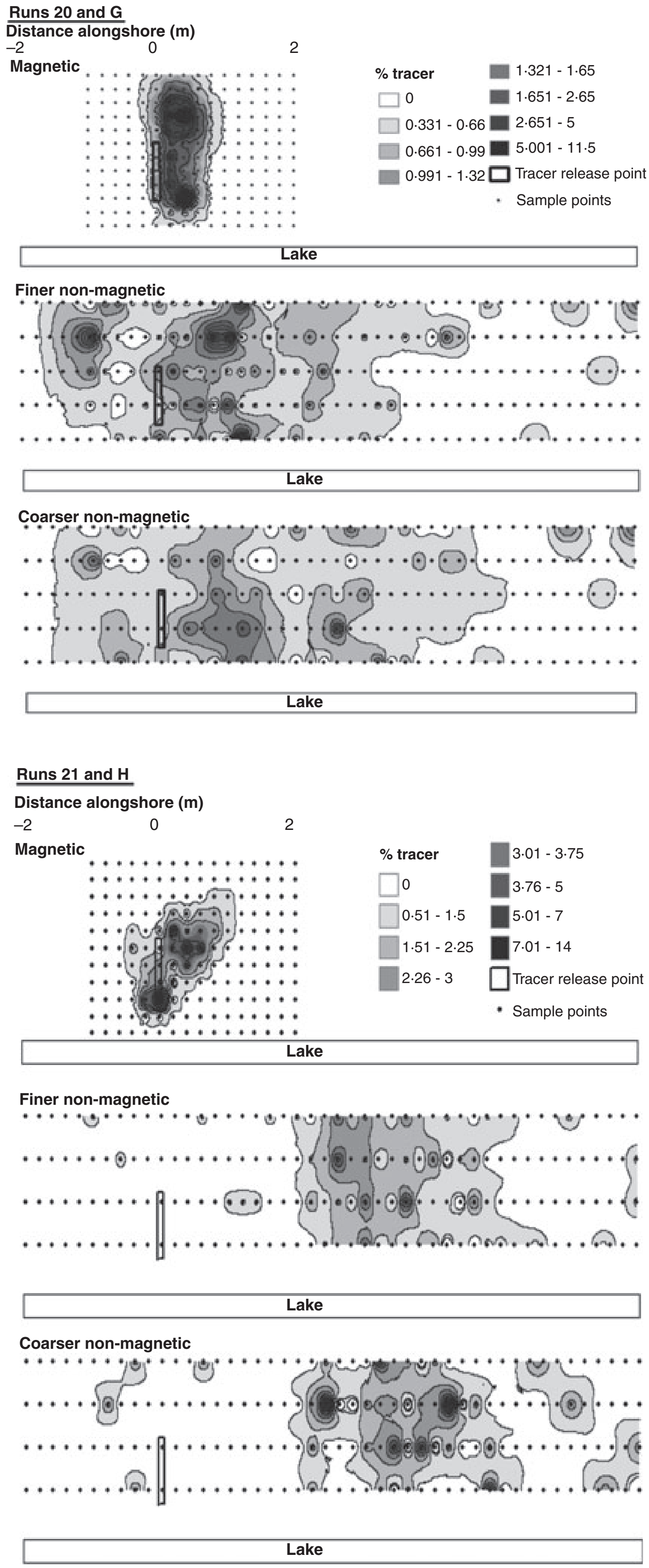

Fig. 5. The movement of magnetic and finer and coarser non-magnetic tracers in two concurrent experiments at Point Pelee. The rectangles show the location where the tracers were released within the measurement grid. Tracer distributions at the end of the sampling period were interpolated between sampling points using an inverse distance-weighted algorithm. The isolines show the fluorescent grains counted in each core as a percentage of the total number of grains counted in all the cores, or the magnetic susceptibility in each cell as a percentage of the total susceptibility for all the cells.

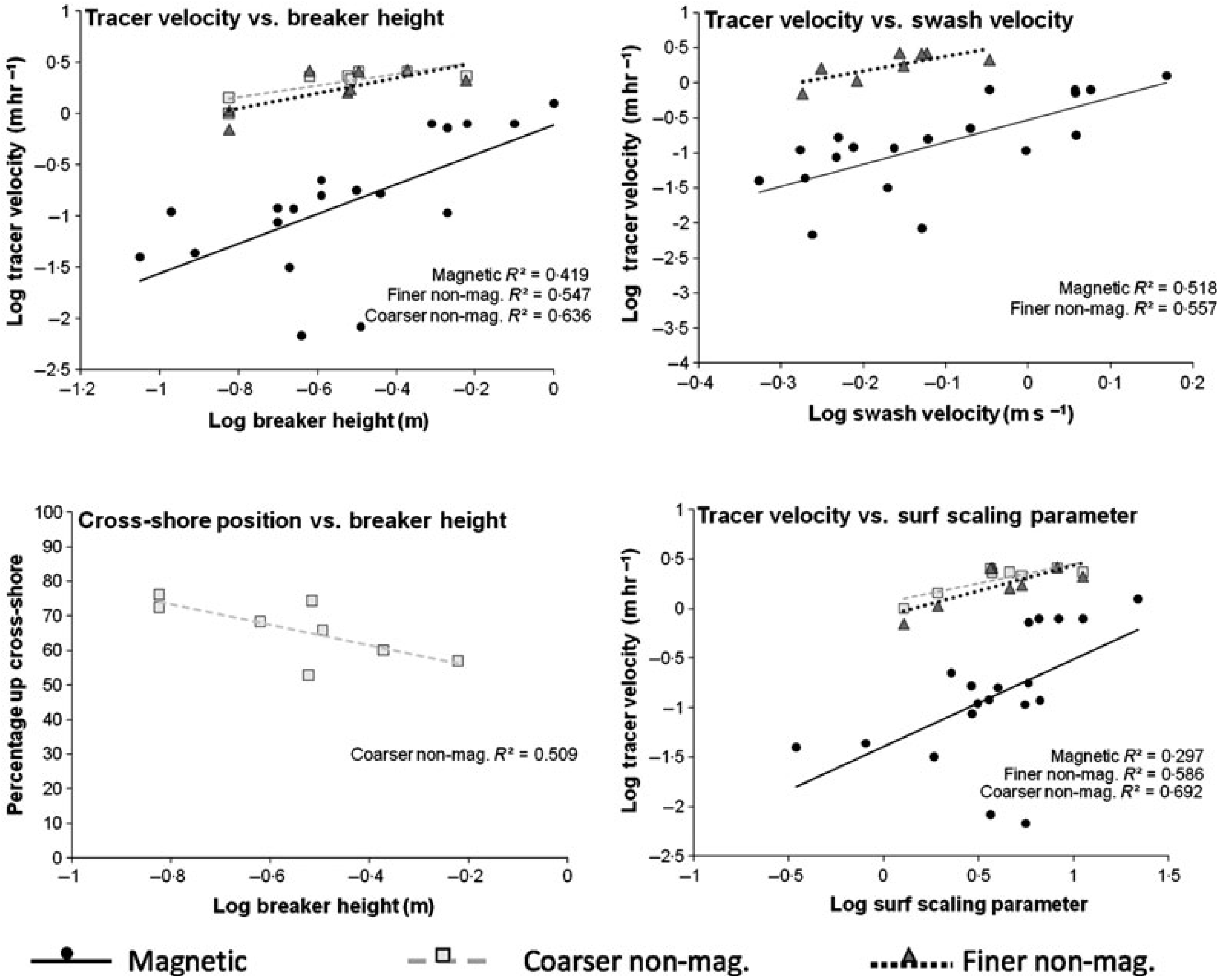

Fig. 6. Significant relationships between tracer movement and aspects of wave and beach conditions.

the swash zone) and the log of the breaker height for the coarser non-magnetic tracers, but they were insignificant for the magnetic and the finer non-magnetic tracers (Fig. 6). There were no significant correlations between cross-shore position and swash uprush velocity, swash angle or wave period for any of the tracers. There were also no significant correlations for any of the tracers between either longshore velocity or cross-shore position and the grain size or gradient of the swash zone.

Several dimensionless parameters have been used to analyse relationships between beach morphology and processes and breaker type, wave runup, and wave reflection and dissipation (Galvin, 1972; Battjes, 1974). The surf scaling parameter (Guza & Bowen, 1975; Guza & Inman, 1975) combines variables describing wave conditions and beach morphology:

$$\varepsilon = \frac{H_b \omega^2}{2g\tan^2\beta}$$

where ε is the surf-scaling parameter, H_b is the breaking wave height, g is the acceleration due to gravity, β is the beach slope and ω, the wave radian frequency, is equal to $2\pi/T$, where T is the wave period. Although the surf-scaling parameter represents the combined effect of a number of variables, correlations between the log of the longshore velocity and the log of the surf scaling parameter were generally only similar or lower than those between the log of the longshore velocity and the log of the breaker height or the log of the swash velocity (Fig. 6). All other correlations with the scaling parameter were insignificant at the 95% probability level, although the correlation between the cross-shore position of the coarser non-magnetic tracers and the log of the scaling parameter was significant at the 90% probability level ($R^2 = 0{\cdot}46$).

The total magnetic susceptibility was recorded through the experiments by totalling the susceptibility in each of the grid cells at various times. Decreasing susceptibility was a measure of the degree to which the small, heavy magnetic minerals sank below and were buried by the larger non-magnetic grains, and was concurrent with the decrease in the longshore velocity of the magnetic tracer centroid. Sudden increases in the magnetic susceptibility did occur in some runs, however, when single waves or a series of waves washed away the non-magnetic grains, re-exposing the magnetic grains below (Fig. 4). None of the correlations between the susceptibility level and wave and swash zone conditions were significant at the 95% probability level. The correlation between the total susceptibility of the magnetic tracers over the first hour of the experiments and the log of the swash grain size was low but significant, however, at the 90% confidence level ($R^2 = 0{\cdot}17$).

Laboratory results

Laboratory experiments showed that magnetic susceptibility decreases with the depth of burial beneath non-magnetic grains. There were rapid decreases in magnetic susceptibility when the magnetic grains were buried under up to a few millimetres of non-magnetic material and slower decreases thereafter, particularly once the magnetic grains were more than *ca* 25 to 40 mm below the surface (Fig. 7A). Rates and depths of burial of the magnetic minerals were much greater when the grain size of the non-magnetic grains was 2·00 to 2·83 mm, *ca* 11 to 16 times larger than the magnetic grains, than when the grain size of the host material was between 0·71 mm and 0·35 mm, from about two to four times larger than the magnetic grains. Burial of

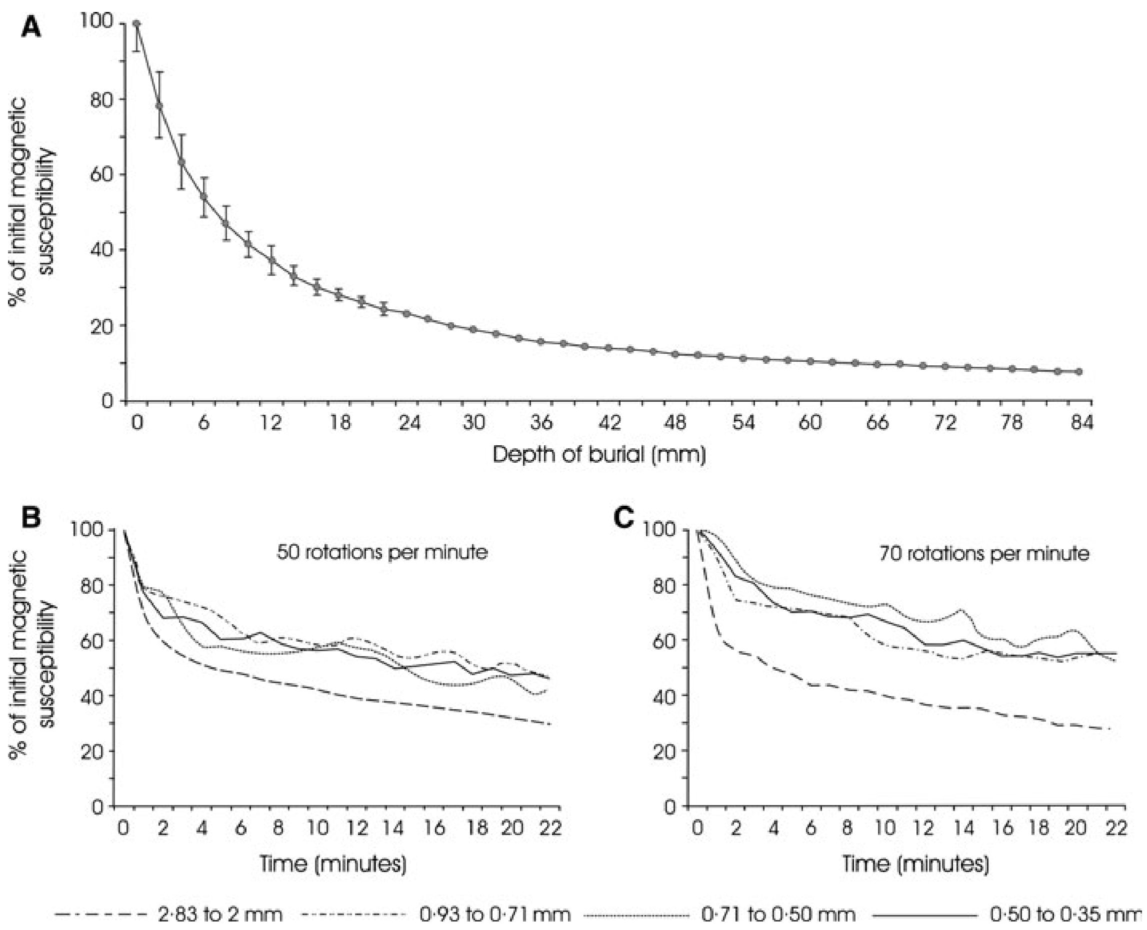

Fig. 7. Laboratory experiments showing decreasing magnetic susceptibility as: (A) a magnetic layer is buried beneath an increasingly thick layer of non-magnetic sand; and (B) and (C) as magnetic grains sink beneath agitated, non-magnetic sand of different grain diameters.

the magnetic grains in the coarsest non-magnetic sand was similar for the two degrees of agitation, but burial in finer non-magnetic sand was more effective at the lower than at the higher level of agitation (Fig. 7B and C). This conclusion is consistent with field experiments in which the magnetic tracers continued to move for a longer period when the breakers were high than when they were low.

DISCUSSION

The experiments showed that small, heavy magnetic minerals are buried rapidly in the swash zone. The magnetic tracers not only travelled less quickly alongshore under low to moderate wave conditions, but there was usually little movement at all after an initial period, generally lasting up to a few hours. In a similar way, magnetic grains tended to move into the upper swash zone before being buried and becoming immobile beneath non-magnetic grains.

Grains with high fall, or settling, velocities do not remain in suspension as long as grains with low fall velocities. Therefore, it is generally assumed that grains with high fall velocities are less easily transported and that neither travel as far or as rapidly as grains with lower fall velocities (suspension sorting). Ferguson & Church (2004) derived a universal equation for grain fall velocity:

$$w_s = \frac{RgD^2}{C_1 v + \sqrt{0 \cdot 75 C_2 RgD^3}}$$

where g is the acceleration due to gravity; D is the grain diameter; C_1 and C_2 are parameters equal, respectively, to 18 and 0·4 for smooth spheres; υ is the kinematic viscosity of the water (1×10^{-6} kg m^{-1} s^{-1} for water at 20°C); and R, the submerged specific gravity of the grain, $=(\rho_g - \rho)/\rho$, where ρ_g is the density of the grain and ρ is the density of the water. Substituting for the density (5200 kg m^{-3}) and mean diameter (178 μm) of the magnetite tracers, and for the corresponding values for the finer (density 2650 kg m^{-3}, mean diameter 209 μm) and coarser (density 2650 kg m^{-3}, mean diameter 483 μm) non-magnetic tracers, suggests that the finer and coarser non-magnetic grains have fall velocities of, respectively, *ca* 0·58 and 1·84 times that of the magnetic grains.

As natural grains are rarely perfectly spherical, several equations have been developed to modify the fall velocity based on the actual shape of the grains (van Rijn, 1989):

$$\frac{w_n}{w_s} = 0 \cdot 808(\mathrm{CSF}) + 0 \cdot 192$$

where w_n is the fall velocity of a non-spherical grain, w_s is the fall velocity of a sphere of the same volume and weight, and CSF (the Corey Shape Factor), is determined from the length of the short (D_s), intermediate (D_i) and long axes (D_l) of the grain:

$$\mathrm{CSF} = \frac{D_s}{\sqrt{D_i D_l}}$$

Microscopic analysis showed that the mean CSF was 0·78 for the magnetic grains and 0·88 and 0·86 for the finer and coarser non-magnetic tracer grains, respectively. Therefore, the actual fall velocities of the finer and coarser non-magnetic tracer grains were, respectively, *ca* 0·64 and 1·99 times that of the magnetic tracers (Table 2).

Heavy magnetic minerals may also be separated from non-magnetic minerals according to different thresholds for the initiation of grain movement (entrainment sorting), which is often

Table 2. Threshold shear stresses and settling velocities.

	Threshold shear stress (Komar & Wang, 1984) (Pa) Host (bed) grain size (μm)				Fall velocity (Ferguson & Church, 2004) (m s^{-1})
	200	300	400	500	
Magnetic tracer	1·61	2·41	3·88	7·32	0·041
Finer non-magnetic tracer	0·61	0·87	1·26	1·92	0·026
Coarser non-magnetic tracer	0·43	0·74	0·89	1·04	0·081
Non-magnetic (330 μm)					0·050
Non-magnetic (2800 μm)					0·327
Non-magnetic bed grains	0·62	0·78	0·91	1·04	

expressed as the minimum shear stress necessary for movement. The critical threshold for sediment entrainment varies with grain size and density, although it is also affected by grain shape and the topography of the bed (Madsen & Grant, 1976; Larsen *et al.*, 1981; Sleath, 1984; Hardisty, 1990). Komar & Wang (1984) provided a semi-empirical expression, which was used by Hughes *et al.* (2000), to determine the critical or threshold shear stress required to pick up sediment from a bed consisting of different grain sizes and densities:

$$\tau_{\mathrm{c}} = 0{\cdot}00515(\rho_{\mathrm{g}} - \rho)gD^{0{\cdot}568}\tan\varphi$$

where D is the mean intermediate diameter of a grain lying on the bed and φ is the angle of repose of the sediment, or the angle between the vertical and a line running between the grain centre and the pivot point. According to Miller & Byrne (1966):

$$\varphi = 61{\cdot}5\left(\frac{D_{\mathrm{i}}}{K}\right)^{-0{\cdot}3}$$

where K is the intermediate diameter of the grains that make up the bed. These equations were used in the present study to calculate the shear stresses needed to initiate movement of the three types of tracer on a bed consisting of grains with diameters ranging from 200 to 500 μm. The results suggest that the critical shear stresses for the finer and coarser grained non-magnetic tracers are, respectively, 0·26 to 0·38 and 0·14 to 0·31 of that determined for the magnetic grains, the lower values corresponding to coarser grains on the bed (Table 2). The Chepil (1959) equation was also modified to consider the effect of differences in grain mineralogy and size on entrainment thresholds. This equation required the pivoting angle to be calculated, for a range of bed grain diameters. Although the shear stresses were a little lower when using the Chepil equation rather than the Komar and Wang equation, the basic relationships between the three types of tracers were similar.

Dispersal of the initial magnetic tracer deposit caused the grains to mix with the more abundant non-magnetic sand in the swash zone. This sand had a mean diameter in the various experiments ranging from *ca* 330 to 2800 μm (Table 1), with corresponding fall velocities 1·23 to 8·02 times that of the magnetic grain tracers. To calculate threshold shear stresses for these swash zone non-magnetic grains, it was assumed that they were sitting on a bed of grains of the same diameter and mineralogy as themselves; this is a reasonable assumption given the numerical dominance and degree of sorting of non-magnetic grains in the swash zone. The Komar & Wang (1984) equation, which can only be used for grains with intermediate diameters <1 mm, showed that for all but the finest non-magnetic grains, threshold shear stresses were much lower than for magnetic grains of the same size (Table 2).

The alongshore movement of the magnetic grains rapidly declined through the experiments because of high threshold shear stresses, shielding by the larger non-magnetic grains (Li & Komar, 1986), and sinking between, and burial beneath, non-magnetic grains. This latter mechanism is consistent with the laboratory experiments and with the progressive decline in total susceptibility. The laboratory experiments suggest that, based on typical decreases of 40 to 60% in the original magnetic susceptibility, the magnetic grains had usually been buried under 4 to 10 mm of non-magnetic grains by the end of each experiment (Fig. 7A).

Both the finer and coarser non-magnetic tracers moved further along the foreshore than the magnetic tracers. The greater movement of the finer non-magnetic tracers was consistent with their lower fall velocities and threshold shear stresses, but the greater movement of the coarser non-magnetic tracers was not consistent with their higher fall velocities (Tables 1 and 2; Fig. 5). The most plausible explanation for the relative transport efficacy of the three tracers is related to the effect of variable grain size and density on the tendency for grain sinking and burial in the swash zone. Decreasing total magnetic susceptibility and the disappearance of the visually distinctive magnetic tracers from the surface testified to the rapid burial of the magnetic tracers in the experiments. Burial of the non-magnetic tracers was more difficult to observe in the field, but the finer non-magnetic tracers were always located deeper in the sediment cores at the end of the experiments than the coarser non-magnetic tracers, with centroid depths ranging, respectively, between 3·2 to 12 mm and 2·4 to 10 mm. This observation suggests that, despite lower masses (0·82 of the magnetic grains), the greater volumes and projected areas of the finer non-magnetic tracer grains (respectively, 1·62 and 1·38 times that of the non-magnetic tracers), together with their lower fall velocities and threshold shear stresses, allowed them to travel faster and further along the beach than the magnetic grains before they too were buried. Despite slightly lower threshold shear stresses, the much higher fall velocities of the coarser than of the finer non-magnetic tracers probably prevented their moving as rapidly alongshore, but because of their greater size they were better able to stay on the surface and to continue moving for longer than the finer non-magnetic and magnetic tracers.

Another factor that would have influenced tracer mobility is their degree of shelter and exposure to the swash within a variable grain population. The generally much larger host grains would have sheltered all the tracer grains, but the effect on transport rates would have been greatest for the smaller magnetic and non-magnetic tracer grains while they were at the beach surface. The amount by which each of the tracers was able to protrude above the surface also affected their exposure to the driving forces, and this was also much greater for the coarser non-magnetic tracers than for either the finer non-magnetic or the magnetic tracers (Fig. 8). Consequently, in addition to differential sinking and burial of the tracers, or kinetic sieving (Clifton, 1969; Tomkins *et al.*, 2010), sheltering and protrusion effects help to explain why the mobility of the coarser non-magnetic tracers was much greater than that of the magnetic tracers, and why they were found at shallower depths and probably continued to move for a longer period, than the finer non-magnetic tracers.

Although differences in transport rates (transport sorting) help to separate magnetic from non-magnetic minerals, the dominance of coarse non-magnetic host grains on the beach, with higher fall velocities than the magnetic grains, shows that placer deposits cannot develop in this area through suspension sorting. Conversely, the much higher threshold shear stresses of the magnetic grains and sheltering by the larger, non-magnetic host grains promote entrainment sorting and cross-shore variations in heavy mineral concentrations and grain sizes. The exposure of beach placers after storms and their association with areas of erosion along the eastern coast of Point Pelee (Hatfield *et al.*, 2010) suggest that strong swash removes consecutive layers of non-magnetic overburden. The finer magnetic grains resist removal, in part because of their higher threshold stresses, but also because of their tendency to sink between the larger, non-magnetic grains; this promotes progressive merging of the seams of magnetic grains and their exposure in the upper swash zone as the non-magnetic grains are removed. The lack of magnetic concentrations in the lower swash zone can be attributed to finer grains that inhibit magnetic grain burial,

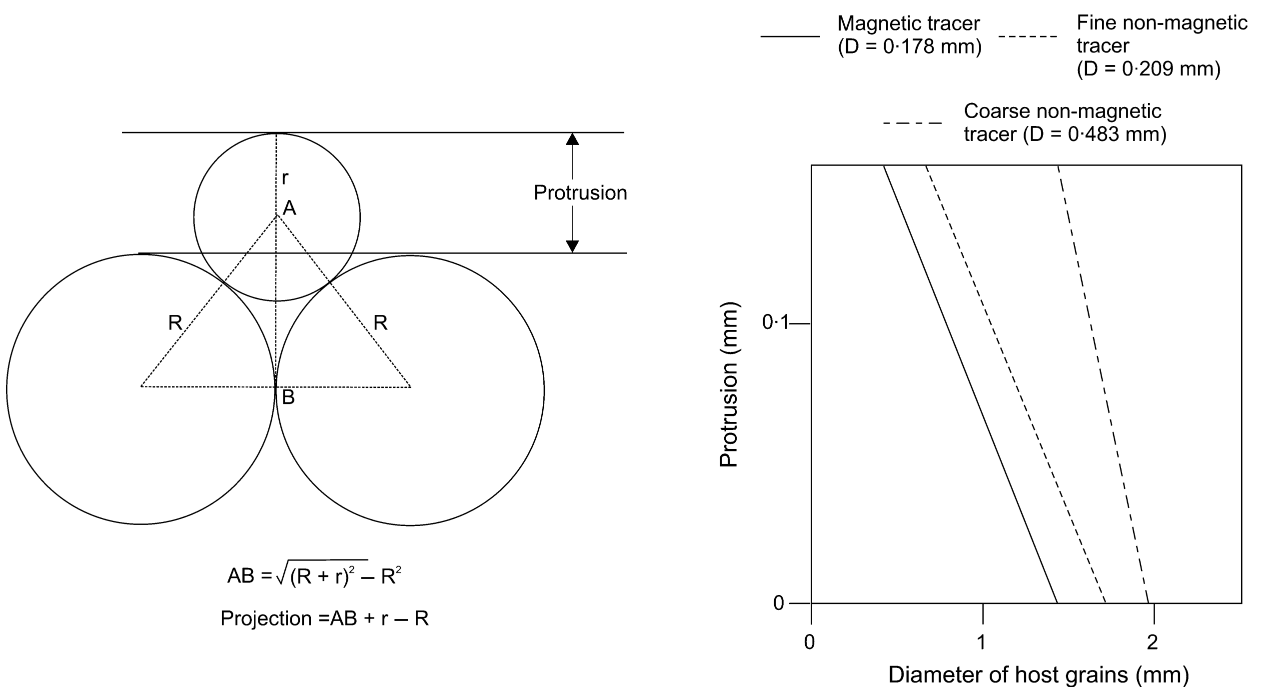

Fig. 8. The radius-dependent relationship between protrusion of a smaller grain above a homogeneous bed of larger grains. There was no protrusion of the smaller above the larger grains when the diameter of the host material was *ca* 1·5 to 2 mm.

stronger swash that is able to remove both the magnetic and non-magnetic material, and the tendency, as demonstrated in this study, for magnetic grains to migrate to, and be buried in, the upper swash zone.

The experiments indicate that heavy magnetic minerals are unable to move along Point Pelee during low to moderate wave conditions, but they also suggest, together with their distribution along this coast (Cioppa *et al.*, 2010; Hatfield *et al.*, 2010), that movement can occur during storms, when removal of the non-magnetic sand concentrates and exposes the magnetic grains. The homogeneity of these magnetic deposits then inhibits grain burial and facilitates longshore and cross-shore transport.

The results of this and similar studies on heavy mineral transport reflect, in part, the specific mineralogical and grain-size characteristics of the beaches, and their wave and tidal regimes. A numerical model suggested that strong flow conditions on a beach near Sydney, Australia, promote shear sorting over entrainment sorting (Hughes *et al.*, 2000). The role of shear sorting in producing placer deposits in the swash zone has been questioned by Tomkins *et al.* (2010), however, who considered kinetic sieving to be the most appropriate mechanism to segregate light and heavy mineral beach sands. In any case, although the Australian beach was similar to Point Pelee, being steeply sloping and consisting of medium-sand, the breaker heights and swash flow intensity were probably much greater than on Lake Erie, which is tideless and dominated by short, locally generated waves. Most other investigators have concluded that entrainment sorting, albeit on gently sloping, fine-grained beaches, is most important in the swash zone (Komar & Wang, 1984; Li & Komar, 1992a,b). In addition to entrainment sorting, the present study has provided additional support for the role of kinetic sieving in the swash zone under fairly gentle flow conditions, and the sheltering of smaller magnetic grains by larger, non-magnetic grains.

Previous work at Point Pelee and in other places has demonstrated that magnetic susceptibility measurements are useful in fingerprinting the source and transport paths for beach sediments. A corollary to the results and conclusions presented in this study, however, is that the distinctive behaviour and episodic movement of magnetic minerals make it difficult to determine longshore transport rates in dominantly non-magnetic sedimentary environments, particularly where the host sand has very different hydrodynamic characteristics. Furthermore, if the stronger wave and swash conditions that concentrate and move magnetic minerals come from different directions than the weaker waves that transport non-magnetic minerals, then magnetic and non-magnetic minerals could actually travel alongshore in opposite directions.

CONCLUSIONS

The main conclusions of this study are as follows:

1 Small, heavy magnetic minerals are buried rapidly beneath non-magnetic grains under low to moderate wave conditions and are unable to move in the longshore or cross-shore direction.

2 Magnetic susceptibility rapidly decreases with the rate and depth of burial of the magnetic minerals.

3 Magnetic grain burial is most effective beneath coarser rather than finer non-magnetic sand and, for the latter sediments, under less rather than more energetic conditions.

4 Magnetic mineral concentrations develop through grain burial under fairly mild conditions, followed by exposure and concentration of consecutive layers during more energetic periods when the non-magnetic grains are eroded from the upper swash zone. Longshore and cross-shore transport of the heavy minerals may then occur during these periods when the homogeneity of the deposits inhibits further burial.

5 Changes in magnetic susceptibility and other magnetic properties can be useful in identifying sediment sources and tracing paths of movement, but the distinct hydrodynamic behaviour of magnetic grains makes it difficult to use them to determine rates of longshore transport in dominantly non-magnetic materials.

ACKNOWLEDGEMENTS

This work was supported by an Ontario Graduate Scholarship to Eric Galloway, Natural Sciences and Engineering Research Council of Canada grants to Alan Trenhaile and Maria Cioppa, and a Post-doctoral Research Fellowship to Robert Hatfield, while at the University of Windsor, by the Canadian Department of Foreign Affairs and International Trade. The authors also thank two anonymous reviewers who provided useful suggestions for improvements to the original manuscript.

REFERENCES

Battjes, J.A. (1974) Surf similarity. *Proc. 14th Coastal Eng. Conf.*, **1,** 466–479.

Booth, C.A., Walden, J., Neal, A. and **Smith, J.P.** (2005) Use of mineral magnetic concentration data as a particle size proxy: a case study using marine, estuarine and fluvial sediments in the Carmarthen Bay area, South Wales, U.K. *Sci. Total Environ.*, **347,** 241–253.

Bryan, K.R., Robinson, A. and **Briggs, R.M.** (2007) Spatial and temporal variability of titanomagnetite placer deposits on a predominantly black sand beach. *Mar. Geol.*, **236,** 45–59.

Chepil, W.S. (1959) Equilibrium of soil grains at the threshold of movement by wind. *Proc. Soil Sci. Soc. Am.*, **23,** 422–428.

Ciavola, P., Taborda, R., Ferreira, O. and **Alveirinho Dias, J.** (1997) Field measurements of longshore sand transport and control processes on a steep meso-tidal beach in Portugal. *J. Coastal Res.*, **13,** 1119–1129.

Cioppa, M.T., Porter, N.J., Trenhaile, A.S., Igokwe, B. and **Vickers, J.** (2010) Beach sediment magnetism and sources: Lake Erie, Ontario, Canada. *J. Great Lakes Res.*, **36,** 674–685.

Clifton, H.E. (1969) Beach lamination: nature and origin. *Mar. Geol.*, **7,** 553–559.

Coakley, J.P. (1980) Postglacial evolution and modern processes at Point Pelee, Lake Erie. In: *The Coastline of Canada* (Ed. S.B. McCann), *Geol. Surv. Can.*, Paper 10-80, 429–437.

Crickmore, M.J. and **Lean, G.H.** (1962) The measurement of sand transport by the time-integration method with radioactive tracers. *Proc. Roy. Soc. London, Ser. A*, **270,** 27–47.

Ferguson, R.I. and **Church, M.** (2004) A simple universal equation for grain settling velocity. *J. Sed. Res.*, **74,** 933–937.

Foster, I.D.L., Albon, A.J., Bardell, K.M., Fletcher, J.L., Jardine, T.C., Mothers, R.J., Pritchard, M.A. and **Turner, S.E.** (1991) High energy coastal sedimentary deposits; an evaluation of depositional processes in southwest England. *Earth Surf. Proc. Land.*, **16,** 341–356.

Frihy, O.E. and **Dewidar, K.M.** (2003) Patterns of erosion/sedimentation, heavy mineral concentration and grain size to interpret boundaries of littoral sub-cells of the Nile Delta, Egypt. *Mar. Geol.*, **199,** 27–43.

Frihy, O.E., Lotfy, M.F. and **Komar, P.D.** (1995) Spatial variations in heavy minerals and patterns of sediment sorting along the Nile Delta, Egypt. *Sed. Geol.*, **97,** 33–41.

Galvin, C.J. (1972) Waves breaking in shallow water. In: *Waves on Beaches* (Ed. R.E. Meyer), pp. 413–456. Academic Press, New York.

Guza, R.T. and **Bowen, A.J.** (1975) The resonant instabilities of long waves obliquely incident on a beach. *J. Geophys. Res.*, **80,** 4529–4534.

Guza, R. and **Inman, D.** (1975) Edge waves and beach cusps. *J. Geophys. Res.*, **80,** 2997–3012.

Hardisty, J. (1990) *Beaches Form and Process*. Unwin Hyman, London, 348 pp.

Hatfield, R.T., Cioppa, M.T. and **Trenhaile, A.S.** (2010) Sediment sorting and beach erosion along a coastal foreland: magnetic measurements in Point Pelee National Park, Ontario, Canada. *Sed. Geol.*, **231,** 63–73.

Hou, B., Frakes, L.A., Alley, N.F. and **Heithersay, P.** (2003) Evolution of beach placer shorelines and heavy-mineral deposition in the eastern Eucla Basin, South Australia. *Aust. J. Earth Sci.*, **50,** 955–965.

Hughes, M.G., Keene, J.B. and **Joseph, R.G.** (2000) Hydraulic sorting of heavy-mineral grains by swash on a medium-sand beach. *J. Sed. Res.*, **70,** 994–1004.

Kamphuis, J.W. (1972) *Progress Report on Point Pelee Beach Study (1970 and 1971) and Marentette Beach Protection Programme*. Ontario Ministry of Lands and Forests, Peterborough, Ontario, Canada, Report DLFS-3.

Kean, W.F. (2004) Distribution of magnetic sands on Lake Michigan beaches near Milwaukee, *Wisconsin. Mich. Acad.*, **35,** 479–492.

Komar, P.D. and **Inman, D.L.** (1970) Longshore sand transport on beaches. *J. Geophys. Res.*, **75,** 5914–5927.

Komar, P.D. and **Wang, C.** (1984) Processes of selective grain transport and the formation of placers on beaches. *J. Geol.*, **92,** 637–655.

Lario, C., Zazo, A.J. and **Plater, I.** (2001) Particle size and magnetic properties of Holocene estuarine deposits from the Donana National Park (SW Iberia): evidence of gradual and abrupt coastal sedimentation. *Z. Geomorph.*, **45,** 33–54.

Larsen, L.H., Sternberg, R.W., Shi, N.C., Marsden, M.A.H. and **Thomas, L.** (1981) Field investigations of the threshold of grain motion by ocean waves and currents. *Mar. Geol.*, **42,** 105–132.

Lees, J.A. and **Pethick, J.S.** (1995) Problems associated with quantitative magnetic sourcing of the Scarborough to Mablethorpe coast, northeast England, U.K. *Earth Surf. Proc. Land.*, **20,** 795–806.

Li, Z. and **Komar, P.D.** (1986) Laboratory measurements of pivoting angles for applications to selective entrainment of gravel in a current. *Sedimentology*, **33,** 413–423.

Li, M.Z. and **Komar, P.D.** (1992a) Longshore grain sorting and beach placer formation adjacent to the Columbia River. *J. Sed. Petrol.*, **62,** 429–441.

Li, M.Z. and **Komar, P.D.** (1992b) Selective entrainment and transport of mixed size and density sands: flume experiments simulating the formation of black-sand placers. *J. Sed. Petrol.*, **62,** 584–590.

Madsen, O.S. and **Grant, W.D.** (1976) Quantitative description of sediment transport by waves. Proc. 15th Coastal Eng. Conf., **2,** 1093–1112.

Maher, B.A., Watkins, S.J., Brunskill, G., Alexander, J. and **Fieldings, C.R.** (2008) Sediment provenance in a tropical fluvial and marine context by magnetic ''fingerprinting'' of transportable sand fractions. *Sedimentology*, **5,** 841–861.

McCubbin, D., Leonard, K.S., Maher, B.A. and **Hamilton, E.I.** (2000) Association of 210Po (210Pb), 239 + 240Pu and 241Am with different mineral fractions of a beach sand at Seascale, Cumbria, UK. *Sci. Total Environ.*, **254,** 1–15.

Miller, R.L. and **Byrne, R.J.** (1966) The angle of repose for a single grain on a fixed rough bed. *Sedimentology*, **6,** 303–314.

Nordstrom, K.F., Jackson, N.L., Allen, J.R. and **Sherman, D.J.** (2003) Longshore sediment transport rates on a microtidal estuarine beach. *J. Waterway, Port, Coast. Ocean Eng.*, **129,** 1–4.

Oldfield, F. and **Yu, L.** (1994) The influence of particle size variations on the magnetic properties of sediments from the north-eastern Irish Sea. *Sedimentology*, **41,** 1093–1108.

Peterson, C.D., Komar, P.D. and **Scheidegger, K.F.** (1986) Distribution, geometry, and origin of heavy mineral placer deposits on Oregon beaches. *J. Sed. Petrol.*, **56,** 67–77.

Plater, A.J. and **Appleby, P.G.** (2004) Tidal sedimentation in the Tees estuary during the 20th century: radionuclide and magnetic evidence of pollution and sedimentary response. *Estuar. Coast. Shelf. Sci.*, **60,** 179–192.

Razjigaeva, N.G. and **Naumova, V.V.** (1992) Trace element composition of detrital magnetite from coastal sediments of northwestern Japan Sea for provenance study. *J. Sed. Res.*, **62,** 802–809.

van Rijn, L.C. (1989) *Handbook Sediment Transport by Currents and Waves*. Delft Hydraulic Report H 461, Delft, The Netherlands.

Rotman, R., Naylor, L., McDonnell, R. and **MacNiocaill, C.** (2008) Sediment transport on the Freiston Shore managed realignment site: an investigation using environmental magnetism. *Geomorphology*, **100,** 241–255.

Sallenger, A.H. (1979) Beach-cusp formation. *Mar. Geol.*, **29,** 23–37.

Skafel, M.G., Bishop, C.T. and **Coakley, J.P.** (1985) *Shore Protection Alternatives for the Marentette Drainage Scheme*. National Water Research Institute Hydraulics Division, Burlington, Canada, Technical Note 85-06.

Sleath, J.F.A. (1984) *Sea Bed Mechanics*. Wiley, Chichester, UK, 358 pp.

Slingerland, R.L. (1977) The effects of entrainment on the hydraulic equivalence relationships of light and heavy minerals in sands. *J. Sed. Petrol.*, **47,** 753–770.

Steidtmann, J.R. (1982) Size density sorting of sand size spheres during deposition from bedload transport and implications concerning hydraulic equivalence. *Sedimentology*, **29,** 877–883.

Tomkins, M.R., Nielsen, P. and **Baldock, T.M.** (2010) Assessment of dispersive pressure as a beach placer mechanism. *Sedimentology*, **57,** 408–417.

Tonk, A. and **Masselink, G.** (2005) Evaluation of longshore transport equations with OBS sensors, streamer traps, and fluorescent tracer. *J. Coastal Res.*, **21,** 915–931.

Trask, C.B. and **Hand, B.M.** (1985) Differential transport of fall-equivalent sand grains, Lake Ontario, New York. *J. Sed. Petrol.*, **55,** 226–234.

Trenhaile, A.S., Lavalle, P.D. and **Lakhan, V.C.** (2000) Canadian landform examples – 39: Point Pelee – a large cuspate foreland on Lake Erie. *Can. Geogr.*, **44,** 191–195.

Wheeler, A.J., Oldfield, F. and **Orford, J.D.** (1999) Depositional and post-depositional controls on magnetic signals from saltmarshes on the northwest coast of Ireland. *Sedimentology*, **46,** 545–558.

White, T.E. and **Inman, D.L.** (1989) Transport determination by tracers B. Application of tracer theory to NSTS experiments. In: *Nearshore Sediment Transport* (Ed. R.J. Seymour), pp. 115–128. Plenum Press, New York.

Yasso, W.E. (1966) Formulation and use of fluorescent tracer coatings in sediment transport studies. *Sedimentology*, **6,** 287–301.

Zhang, W., Yu, L., Lu, M., Hutchinson, S.M. and **Feng, H.** (2007) Magnetic approach to normalizing heavy metal concentrations for particle size effects in intertidal sediments in the Yangtze Estuary, China. *Environ. Pollut.*, **147,** 238–244.

Manuscript received 26 July 2011; revision accepted 26 January 2012